

Louisiana Coastal Area (LCA), Louisiana

Ecosystem Restoration Study

November 2004

Final

Appendix D - Louisiana Gulf Shoreline Restoration Report

**LOUISIANA COASTAL AREA (LCA), LOUISIANA
ECOSYSTEM RESTORATION STUDY**

APPENDIX D

LOUISIANA GULF SHORELINE RESTORATION REPORT

TABLE OF CONTENTS

CHAPTER D.1	REGIONAL GEOLOGY OF SOUTHERN LOUISIANA	D-1
1.1	SUMMARY	D-1
1.2	INTRODUCTION	D-1
1.3	CREATION AND EVOLUTION OF THE NORTH-CENTRAL GULF OF MEXICO BASIN.....	D-3
1.4	HOLOCENE EVOLUTION AND PHYSIOGRAPHIC PROVINCES	D-5
1.4.1	Formation of the Deltaic and Chenier Plains.....	D-5
1.4.2	Deltaic Plain.....	D-5
1.4.3	Chenier Plain.....	D-9
1.5	CONCLUSION.....	D-12
CHAPTER D.2	PHYSICAL PROCESSES ALONG THE LOUISIANA COAST	D-13
2.1	SUMMARY	D-13
2.2	INTRODUCTION	D-13
2.3	WAVES... ..	D-14
2.3.1	Deepwater Waves	D-14
2.3.2	Nearshore Waves	D-16
2.4	STORMS.....	D-19
2.4.1	Cold Fronts.....	D-19
2.4.2	Hurricanes and Tropical Storms	D-21
2.5	TIDES	D-27
2.6	SEA LEVEL RISE AND SUBSIDENCE	D-29

2.7	TIDAL INLETS AND TIDAL PRISM DYNAMICS.....	D-30
2.8	ESTUARINE CIRCULATION	D-33
2.9	LONGSHORE SEDIMENT TRANSPORT	D-34
2.9.1	West Louisiana - Holly Beach (Calcasieu Sabine).....	D-36
2.9.2	Isles Dernieres.....	D-36
2.9.3	Timbalier Islands	D-37
2.9.4	Chandeleur Islands.....	D-37
2.9.5	Barataria Bay	D-37
2.10	CROSS-SHORE SEDIMENT DISPERSAL.....	D-38

CHAPTER D.3 CHANGES IN LOUISIANA’S SHORELINE: 1855–2002..... D-41

3.1	SUMMARY	D-41
3.2	INTRODUCTION	D-41
3.3	PREVIOUS COASTAL EROSION RESEARCH	D-43
3.3.1	U.S. Army Corps of Engineers	D-43
3.3.2	Louisiana Attorney General.....	D-44
3.3.3	Louisiana Department of Transportation and Development.....	D-48
3.3.4	Louisiana Department of Natural Resources	D-48
3.3.5	U.S. Geological Survey.....	D-50
3.3.6	Environmental Protection Agency	D-53
3.4	SHORELINE CHANGES: 1855 TO 2002.....	D-53
3.4.1	Methodology	D-53
3.4.2	Shoreline Reaches.....	D-59
3.5	CONCLUSION.....	D-92

CHAPTER D.4 WAVE AND STORM PROTECTION PROVIDED BY LOUISIANA’S GULF SHORELINE: BARRIER ISLANDS AND SHELL REEFS D-94

4.1	SUMMARY	D-94
4.2	BARRIER ISLANDS	D-94
4.2.1	Introduction.....	D-94
4.2.2	Numerical Wave Modeling.....	D-95
4.2.3	Extreme Events	D-96

4.2.4	The Significance of Storm Surge.....	D-96
4.3	SHELL REEFS	D-102
4.3.1	Introduction.....	D-102
4.3.2	Influence of the Atchafalaya River on Coastal Processes	D-104
4.3.3	Shell Reef Interaction with Wave Behavior	D-108

CHAPTER D.5 USING MODELS TO EVALUATE THE EFFECT OF BARRIER ISLANDS ON ESTUARINE HYDRODYNAMICS AND HABITATS: A NUMERICAL EXPERIMENT D-112

5.1	SUMMARY	D-112
5.2	INTRODUCTION	D-112
5.3	GOALS AND OBJECTIVES	D-113
5.4	USE OF MODELING IN ENVIRONMENTAL MANAGEMENT	D-113
5.5	DYNAMIC MODELS IN ESTUARIES	D-114
5.5.1	Dynamic Estuarine Models in Coastal Louisiana.....	D-114
5.6	METHODS	D-115
5.6.1	Hydrodynamic Module	D-117
5.6.2	Desktop Habitat Type Module.....	D-118
5.6.3	Faunal Habitat Suitability Module.....	D-118
5.7	RESULTS – HYDRODYNAMIC MODULE.....	D-120
5.7.1	Salinity	D-122
5.7.2	Temperature	D-123
5.7.3	Basin Circulation	D-123
5.7.4	Tidal Prism.....	D-123
5.8	RESULTS – DESKTOP HABITAT CHANGE MODULE.....	D-134
5.9	RESULTS – FAUNAL HABITAT SUITABILITY MODULE	D-134
5.10	DISCUSSION	D-142

CHAPTER D.6 RESTORATION TOOLS FOR LOUISIANA’S GULF SHORELINE..... D-143

6.1	SUMMARY	D-143
6.2	APPLICATIONS AND USES OF COASTAL MODELS.....	D-143
6.2.1	INTRODUCTION	D-143

6.2.2	Analytic Desktop Models	D-144
6.2.3	Existing Analytical and Numerical Shoreline Change Models	D-145
6.2.4	Cross-Shore Profile Evolution Models	D-148
6.3	BASIC CONCEPTS OF SHORELINE AND PROFILE MODELING.....	D-149
6.3.1	Closure Depth	D-149
6.3.2	Equilibrium Profile	D-152
6.3.3	Wave Analysis	D-154
6.3.4	Effect of Offshore Sand Removal on Coastal Wave Climate.....	D-155
6.3.5	Wave Effects on the Coast.....	D-155
6.3.6	Wave Model Selection and Validation	D-155
6.3.7	Statistical Considerations in Barrier Island Restoration	D-156
6.3.8	Calibration and Verification of Coastal Models	D-157
6.4	COASTAL SEDIMENT APPLICATIONS AND COSTS	D-157
6.4.1	Applications of Model Concepts to the Design of BEACH Nourishment	D-162
6.4.2	Project Cost Analysis.....	D-165
6.4.3	Estimate of Dredging Costs	D-167
6.5	COASTAL STRUCTURE APPLICATIONS	D-169
6.5.1	Summary	D-169
6.5.2	Seawalls	D-169
6.5.3	Revetments.....	D-171
6.5.4	Terminal Groins	D-172
6.5.5	Groins.....	D-174
6.5.6	Breakwaters.....	D-175
6.5.7	Jetties.....	D-177
6.6	VEGETATIVE PLANTINGS	D-179
6.6.1	Summary	D-179
6.6.2	Dune Habitat	D-180
6.6.3	Swale Habitat	D-182
6.6.4	Back-barrier Marsh Habitat	D-183
6.6.5	Coastal Plant Technology	D-183
6.6.6	Formula for Vegetation Restoration Success.....	D-185

CHAPTER D.7	GULF SHORELINE SEDIMENT RESOURCES.....	D-187
7.1	SUMMARY	D-187
7.2	INTRODUCTION	D-187
7.3	DEPOSITIONAL ENVIRONMENTS OF SEDIMENT RESOURCES.....	D-189
7.3.1	Fluvial Environments.....	D-190
7.3.2	Channel-fill Deposits	D-191
7.3.3	Deltaic Environments.....	D-192
7.3.4	Distributary Mouth-bar Deposits	D-192
7.3.5	Shoreline Systems.....	D-193
7.3.6	Re-curved Spits, Barrier Systems, Beach Ridges, and Cheniers	D-193
7.3.7	Tidal Inlets and Tidal Deltas.....	D-193
7.4	OFFSHORE SAND SHOALS.....	D-194
7.4.1	Trinity Shoal	D-195
7.4.2	Ship Shoal	D-195
7.4.2.1	Shoal Crest.....	D-195
7.4.2.2	Shoal Front.....	D-196
7.4.2.3	Shoal Base.....	D-196
7.4.3	Outer Shoal	D-197
7.4.4	St. Bernard Shoals.....	D-197
7.5	SEDIMENT RESOURCE RESEARCH AND REGIONAL DISTRIBUTION	D-197
CHAPTER D.8	BEST MANAGEMENT PRACTICES FOR COSTAL RESTORATION IN LOUISIANA.....	D-203
8.1	ADAPTIVE MANAGEMENT.....	D-203
8.1.1	Summary	D-203
8.1.2	Preliminary Conceptual Model	D-203
8.1.3	Design and Construction.....	D-204
8.1.4	Monitoring and Evaluation	D-204
8.1.5	Feedbacks Between Monitoring and Design	D-204
8.2	BARRIER ISLANDS	D-204
8.2.1	Summary	D-204
8.2.2	Design and Construction Considerations for Gulf Shoreline Restoration	D-205

8.2.2.1	Development of a Conceptual Model and Regional Sediment Budget	D-205
8.2.2.2	Sand Depth of Closure	D-205
8.2.2.3	Templete	D-205
8.2.2.4	Advance Fill.....	D-206
8.2.2.5	Monitoring and Maintenance	D-206
8.2.2.6	Two Side Nourishment of Barrier Islands	D-206
8.2.2.7	Breach and Inlet Closures	D-212
8.2.2.8	Restoration Priority	D-214
8.2.2.9	Mainland and Bay Shorelines	D-214
8.2.3	Design, Construction, and Consolidation Considerations for Marsh Restoration	D-214
8.2.4	Construction/Plans and Specs.	D-214
8.2.5	Review of the Barrier Island Feasibility Study Restoration Strategies.....	D-216
8.2.6	Use of Channel Maintenance Sediments for Barrier Island Restoration	D-216
8.3	BEST MANAGEMENT PRACTICES FOR COASTAL STRUCTURES	D-217

CHAPTER D.9 PROJECT DESIGN AND CONSTRUCTION TEMPLATES..... D-222

9.1	SUMMARY.....	D-222
9.2	INTRODUCTION.....	D-222
9.3	CROSS-SHORE, GULF LANDWARD.....	D-224
9.3.1	Dune Height and Marsh Platform Width.....	D-225
9.3.2	Retreat Mechanisms and Island Height.....	D-227
9.3.3	Marsh Platform.....	D-229
9.4	CROSS-SHORE, GULF SEAWARD.....	D-229
9.4.1	Presence or Absence of Dunes.....	D-230
9.4.2	Presence or Absence of Beach Berm.....	D-231
9.4.3	Shallow Versus Deep Depth of Closure (Doc).....	D-233

CHAPTER D.10 REGIONAL STRATEGIES FOR COASTAL RESTORATION IN LOUISIANA: BARRIER ISLANDS AND MAINLAND SHORELINES..... D-234

10.1	SUMMARY.....	D-234
10.2	INTRODUCTION.....	D-234

10.3	SUBPROVINCE 1, CHANDELEUR ISLANDS.....	D-238
10.3.1	Geographical Location.....	D-238
10.3.2	Geological/ Geomorphological Setting.....	D-238
10.3.3	Historical Information (Retreat Rates, Inlet Openings, Human Use).....	D-240
10.3.4	Human Use and Infrastructures.....	D-241
10.3.5	Special and Unique Aspects of the Chandeleur Islands.....	D-241
10.3.6	Island Dimensions.....	D-241
10.3.7	Identification of Best Strategies for the Area.....	D-242
10.3.8	Approximate Volumetric Requirements.....	D-243
10.3.9	Potential Sand Sources for the Area.....	D-244
10.3.10	Research and Monitoring Needs and Further Plan Development.....	D-244
10.4	SUBPROVINCE 2, PLAQUEMINES SHORELINE.....	D-244
10.4.1	Geographical Location.....	D-244
10.4.2	Unique Aspects.....	D-246
10.4.3	Island Dimensions.....	D-246
10.4.4	Retreat Rates, Inlet Openings and Back Bay Areas.....	D-247
10.4.5	Human Uses and Infrastructures.....	D-249
10.4.6	Identification of Best Strategies for the Area.....	D-249
10.4.7	Approximate Volumetric Requirements.....	D-251
10.4.8	Potential Sand Sources for the Area.....	D-252
10.4.9	Research Monitoring Needs and Further Plan Development.....	D-252
10.5	SUBPROVINCE 2, LAFOURCHE SHORELINE (CAMINADA-MOREAU HEADLAND AND GRAND ISLE).....	D-252
10.5.1	Geographical Location.....	D-252
10.5.2	Geological Heritage and General Geomorphology.....	D-253
10.5.3	Retreat Rates, Acreage Loss, and Inlet Openings.....	D-254
10.5.4	Current Human Uses and Infrastructures.....	D-255
10.5.5	Island Dimensions.....	D-257
10.5.6	Identification of Best Strategies for the Area.....	D-258
10.5.7	Approximate Volumetric Requirements.....	D-259
10.5.8	Research and Monitoring Needs.....	D-260
10.6	SUBPROVINCE 3, TIMBALIER ISLANDS.....	D-260
10.6.1	Geographical Location.....	D-260

10.6.2 Geological Heritage and General Geomorphology.....	D-260
10.6.3 a Retreat Rates, Acreage Loss and Inlet Openings.....	D-262
10.6.4 Human Uses and Previous Interventions.....	D-263
10.6.5 Island Dimensions.....	D-263
10.6.6 Identification of Best Strategies for the Area.....	D-264
10.6.7 Approximate Volumetric Requirements.....	D-266
10.6.8 Potential Sand Sources for the Area.....	D-267
10.6.9 Research and Monitoring Needs and Further Plan Development.....	D-267
10.7 SUBPROVINCE 3, ISLES DERNIERES.....	D-267
10.7.1 Geographical Location.....	D-267
10.7.2 Geological Heritage and General Geomorphology.....	D-268
10.7.3 Retreat Rates, Acreage Loss and Inlet Openings.....	D-269
10.7.4 Island Dimensions.....	D-271
10.7.5 Human Usage and Previous Restoration Projects.....	D-272
10.7.6 Identification of Best Management Strategies for the Area.....	D-275
10.7.7 Determination of Volumetric Requirements.....	D-277
10.7.8 Potential Sand Sources.....	D-278
10.7.9 Research and Monitoring Needs.....	D-278
10.8 SUBPROVINCE 3, POINT AU FER TO FRESH WATER BAYOU.....	D-279
10.8.1 Geographical Location.....	D-279
10.8.2 Geological Inheritance and General Geomorphology.....	D-279
10.8.3 Retreat Rates, Acreage Loss, and Inlet Openings.....	D-280
10.8.4 Unique Characteristics.....	D-281
10.8.5 Island Dimensions (Slopes, Heights).....	D-284
10.8.6 Human Use and Recent Projects.....	D-284
10.8.7 Identification of Best Strategies for the Area.....	D-285
10.9 SUBPROVINCE 4., EASTERN CHENIER PLAIN (FRESHWATER BAYOU TO CALCASIEU PASS).....	D-287
10.9.1 Geographical Location.....	D-288
10.9.2 Geological Inheritance and General Geomorphology.....	D-288
10.9.3 Retreat Rates.....	D-288
10.9.4 Human Use and Previous Projects.....	D-289
10.9.5 Identification of Best Strategies for the Area.....	D-289

10.9.6 Volumetric Densities.....	D-291
10.9.7 Potential Sand Sources.....	D-291
10.10 SUBPROVINCE 4, CALCASIEU-SABINE SHORELINE.....	D-292
10.10.1 Geographical Location.....	D-292
10.10.2 Geological Inheritance and General Geomorphology.....	D-292
10.10.3 Shoreline Change Rates.....	D-292
10.10.4 Current Human Use and Previous Projects.....	D-293
10.10.5 Identification of Best Strategies for the Area.....	D-294
10.10.6 Determination of Volumetric Requirements and Costs.....	D-296
10.10.7 Potential Sand Sources.....	D-296
LITERATURE CITED.....	D-298

LIST OF FIGURES

Figure D.1 1. Map of study area showing the Mississippi River Delta region of the north-central Gulf of Mexico.	D-2
Figure D.1 2 Geographic distribution and chronology of Holocene Mississippi River delta	D-6
Figure D.1-3. Three-stage conceptual model detailing the genesis and evolution of transgressive depositional systems along the Mississippi River Deltaic Plain	D-7
Figure D.1-4. Graph of the delta cycle showing the growth and decay of individual delta lobes through processes of fluvial switching and relative sea level rise (from Roberts 1997).	D-9
Figure D.1-5. Regional geomorphologic framework of the southwestern Louisiana Chenier Plain.	D-10
Figure D.1-6. Conceptual diagram showing the processes contributing to the construction of the southwestern Louisiana Chenier Plain	D-11
Figure D.2-1. Sites of deepwater wave gages (NOAA stations, solid circles and nearshore WAVCIS station (open circle).	D-14
Figure D.2-2. Wave (right) and wind (left) roses for data collected at WAVCIS station (CSI-5) showing seasonal effects during summer (top) and winter (bottom).	D-17
Figure D.2-3. Time series of wave height data from WAVCIS station CSI-5 during summer (upper) and winter (lower) months.	D-18
Figure D.2-4. Types of cold fronts produced by different weather systems.	D-19
Figure D.2-5. Weather maps illustrating the end member types of Gulf Coast cold front passages	D-20
Figure D.2-6. Wind, wave, and tidal elevation data measured at a production platform off the delta coast.	D-20
Figure D.2-7. Hurricane storm tracks in the Gulf of Mexico for the 1886-1996 period (Stone et al. 2003)	D-21
Figure D.2-8. Graph showing distribution of hurricanes and tropical storms along the Louisiana coast from 1901 to 1996 (from Stone et al. 1997).	D-22
Figure D.2-9. Satellite view of hurricane Georges before landfall on September 27, 1998 off coastal Louisiana.	D-23
Figure D.2-10. Tracks and Category Status of Hurricane 1947, Betsy, Camille, and Georges.	D-24
Figure D.2-11. Storm Surge produced by hurricanes 1947, Betsy, Camille, and Georges, at the Gulfport gauge.	D-25
Figure D.2-12. Tracks for Tropical Storm Isidore and Hurricane Lili (from Stone and Sheremet 2003).	D-26
Figure D.2-13. Water levels as a result of Tropical Storm Isidore and Hurricane Lili (from Stone and Sheremet 2003).	D-26

Figure D.2-14. Significant Wave Heights as a result of Tropical Storm Isidore and Hurricane Lili (from Stone and Sheremet 2003).	D-27
Figure D.2-15. Lidar images post-Hurricane Lili showing net accretion and erosion.	D-27
Figure D.2-16. Typical tidal signature along coastal Louisiana from west (top) to east (bottom).	D-28
Figure D.2-17. Tide Gauge at Eugene Island.	D-29
Figure D.2-18. Tide Gauge at Grande Isle.	D-30
Figure D.2-19. Map of subsidence rates in North America.	D-30
Figure D.2-20. Map of Barataria Basin land loss/gain.	D-32
Figure D.2-21. West to east cross-sections at Caminada Pass, Barataria Pass, Pass Abel, Quatre Bayou, showing inlet changes since 1890.	D-32
Figure D.2-22. Location map of Louisiana coastal waters.	D-33
Figure D.2-23. Longshore sediment transport estimates in coastal Louisiana	D-35
Figure D.2-24. Calculated longshore transport rates in west Louisiana under fair weather D-conditions (Underwood et al. 1999).	D-36
Figure D.2-25. Longshore sediment transport estimates for the Chandeleur Islands using numerical wave modeling (from Ellis 1998).	D-38
Figure D.2-26. Oblique aerial of Raccoon Island looking west (Photograph taken by G.W. Stone in 2000).	D-39
Figure D.2-27. Sea floor changes from 1878 to 1989 in coastal Louisiana (from List et al. 1989).	D-40
Figure D.3- 1. A map of the six delta complexes within the Holocene Mississippi River delta plain.	D-42
Figure D.3- 2. A geologic map depicting the geomorphology of the Mississippi River Chenier Plain in western Louisiana (Penland et al. 1990).	D-43
Figure D.3- 3. The first map to depict coast-wide shoreline changes between 1812 and 1954 for the eastern half of Louisiana by Morgan and Larimore (1957) for the Louisiana Attorney General.	D-46
Figure D.3- 4. The first map to depict coast-wide shoreline changes between 1812 and 1954 for the western half of Louisiana by Morgan and Larimore (1957) for the Louisiana Attorney General.	D-47
Figure D.3- 5. Morgan and Morgan (1983) updated the original Morgan and Larimore (1957) study for the LA Attorney General from 1932 – 1954 to 1932 – 1969.	D-48
Figure D.3- 6. Shoreline change maps for the Timbalier Islands for 1887 to 1988 and 1978 to 1988 from the USGS Louisiana Barrier Island Erosion Study— “Atlas of Shoreline Changes for 1853 to 1989” (Williams et al. 1992; McBride et al. 1992).	D-51

Figure D.3- 7. A seafloor change map for the Timbalier Islands from the 1930s to the 1980s from the USGS Louisiana Barrier Island Erosion Study—“Atlas of Seafloor Changes for 1978 to 1989” (List et al. 1994).	D-52
Figure D.3- 8. Map depicting long-term shoreline changes in Louisiana by the Coastal Erosion Subcommittee of the Environmental Protection Agency’s Gulf of Mexico program (Penland 1996).	D-54
Figure D.3- 9. A diagram of the 34 coast-wide shoreline reaches in Louisiana with the average long-term shoreline change rate between 1855 and 1989	D-60
Figure D.3- 10. A diagram of the 34 coast-wide shoreline reaches in Louisiana with the average short-term shoreline change rate between 1985 and 2002.	D-62
Figure D.3- 11. Historical modern map overlays for the Isles Dernieres for 1887 –1988 and 1988–2002.	D-71
Figure D.3- 12. Graph of the area changes and area rate of change for the Isles Dernieres between 1887 and 2002.	D-72
Figure D.3- 13. A time-series documenting the historical area changes in Raccoon Island (TE-25) between 1978 and 2002.	D-73
Figure D.3- 14. A time-series documenting the historical area changes in Whiskey Island (TE-27) between 1978 and 2002.	D-74
Figure D.3- 15. A time-series documenting the historical area changes in Trinity Island (TE-24) between 1978 and 2002.	D-75
Figure D.3- 16. A time-series of the area of East Island from 1978 to 2002.	D-76
Figure D.3- 17. Historical map overlays for the Timbalier Islands for 1887 - 1988 and 1988 - 2002.	D-77
Figure D.3- 18. Graph of the area change and area rate of change for the Timbalier Islands between 1887 and 2002.	D-79
Figure D.3- 19. Historical and modern map overlays for the Caminada-Moreau Coast from 1887 - 1988 and 1988 – 2002.	D-81
Figure D.3- 20. Historical and modern map overlays for Grand Isle from 1887 – 2002. Grand Isle is Shoreline Reach 23.	D-82
Figure D.3- 21. Graphs of the historical area of Grand Isle between 1887 and 2002 with the area rate of change	D-83
Figure D.3- 22. Historical and modern map overlays for the Plaquemine barrier shoreline between 1884 – 12988 and 1988 – 2002.	D-84
Figure D.3- 23. Historical and modern map overlays for the West and East Grand Terre Islands between 1884-1988 and 1988-2002.	D-85
Figure D.3- 24. Graphs of the historical area of Grand Terre between 1884 and 2002	D-87
Figure D.3- 25. Historical and modern map overlays for Shell Island along the Plaquemine shoreline between 1884 – 1988 and 1988 – 2002.	D-88

Figure D.3- 26. Graphs of the historical area of Shell Island between 1884 and 2002. Shell Island has a long-term area loss rate of -2.2 ac/yr and a short-term loss rate of -8.3 ac/yr.	D-89
Figure D.3- 27. Historical and modern map overlays of the Southern Chandeleur Islands consisting of Breton, Grand Gossier, and Curlew Islands between 1869 and 2002.	D-90
Figure D.3- 28. Historical and modern map overlays for North Chandeleur Island dated 1855 and 1988.	D-91
Figure D.3- 29. Graph of the historical area of the Chandeleur Islands between Breton Island and Hewes Point.	D-93
Figure D.4- 1. Numerically derived wave field under fairweather, deep-water wave conditions along the Timbalier islands and Fourchon.	D-95
Figure D.4- 2. MODIS image showing the location of various ocean-observing stations relative to storm tracks of TS Isidore and Hurricane Lili.	D-97
Figure D.4- 3. Time series of significant wave heights (m) at five locations from the central GOM to Terrebonne Bay along the path of TS Isidore.	D-97
Figure D.4- 4. Water/surge levels during Tropical Storm Isidore and Hurricane Lili measured in shallow water off Timbalier Island (CSI 5) and in Terrebonne Bay (CSI 11).	D-98
Figure D.4- 5. Left: Coastal configuration in 1950 where the study site had ~ 1.09 million acres of land. Middle:	D-99
Figure D.4- 6. Distribution of maximum surge elevation and significant wave height across the study site for the 1950 scenario (from Stone et al. 2003).	D-100
Figure D.4- 7. Maximum storm surge elevation and significant wave height distribution across the study site for the 1990s scenario (from Stone et al. 2003).	D-101
Figure D.4- 8. Maximum storm surge elevation and significant wave height for the study area in the 2020 scenario (from Stone et al. 2003).	D-101
Figure D.4- 9. Map of the study site from Point Au Fer to the eastern flank of the Chenier Plain.	D-102
Figure D.4- 10. Surface area change of maximum surge (A), maximum significant wave height (B) and the composite of surge and wave height (C). Rate of surface area change of maximum surge (D), maximum significant wave height (E) and the composite of surge and wave height (F). (from Stone et al. 2003).	D-103
Figure D.4- 11. Terra Modis image of Atchafalaya Bay showing the infusion of fine grained sediment into the bay and Gulf of Mexico	D-105
Figure D.4- 12. Upper: Time series of significant wave height (12/02-01/03) at a WAVCIS station (CSI 3) located on the 5 m isobath off Marsh Island. Lower: Time series of sustained wind speed recorded at CSI 3.	D-106
Figure D.4- 13. Comparison of significant wave height at CSI 3 and CSI 5 where 3 are located in an offshore area dominated by mud, and 5 is more sandy.	D-107

Figure D.4- 14. Bathymetric map of the Atchafalaya Bay and inner shelf prior to the gradual dredging of oyster reefs.	D-108
Figure D.4- 15. Bathymetric map of the inner shelf and Atchafalaya Bay area after removal of virtually all oyster reefs for commercial use.	D-109
Figure D.4- 16. Distribution of wave height modeled using SWAN for conditions prior to oyster reef removal. Conditions are indicative of fair-weather waves.	D-109
Figure D.4- 17. Distribution of wave height modeled using SWAN for conditions after oyster reef removal. Conditions are indicative of fair-weather waves.	D-110
Figure D.4- 18. Difference in wave height due to oyster shell reef removal.	D-110
Figure D.5-1. Initial habitat distribution for scenario analysis.	D-116
Figure D.5-2. Measured and predicted land loss rates in Caernarvon watershed (modified from Coast 2050, Appendix D).	D-117
Figure D.5-3. Mean annual salinity distribution along a south-north transect, with lateral variability (Islands at 14 km)	D-121
Figure D.5-4. Mean annual salinity distribution along a south-north transect, with lateral variability (Islands at 7 km)	D-121
Figure D.5-5. Mean annual salinity distribution along a south-north transect, with lateral variability (No Islands).	D-121
Figure D.5-6. Mean annual longitudinal distribution of salinity differential (14 - 7 km). Negative values indicate higher salinity at specific locations in the estuary for 7 km scenario vs 14 km scenario.	D-122
Figure D.5-7. Mean annual longitudinal distribution of salinity differential (14 - 0 km). Negative values indicate higher salinity at specific locations in the estuary for no islands scenario vs 14 km scenario.	D-122
Figure D.5-8. Seasonal salinity differential distribution for the period of December through February (case: 14 - 7 km).	D-125
Figure D.5-9. Seasonal salinity differential distribution for the period of December through February (case: 14 - 0 km).	D-126
Figure D.5-10. Seasonal salinity differential distribution for the period of March through May (case: 14 - 7 km).	D-127
Figure D.5-11. Seasonal salinity differential distribution for the period of March through May (case: 14 - 0 km).	D-128
Figure D.5-12. Seasonal salinity differential distribution for the period of June through August (case: 14 - 7 km).	D-129
Figure D.5-13. Seasonal salinity differential distribution for the period of June through August (case: 14 - 0 km).	D-130
Figure D.5-14. Seasonal salinity differential distribution for the period of September through November (case: 14 - 7 km).	D-131

Figure D.5-15. Seasonal salinity differential distribution for the period of September through November (case: 14 - 0 km).	D-132
Figure D.5-16. Inlet flow comparisons over several tidal cycles for the 14 km and 7 km cases. Note that the total flow through the inlets is proportional to the surface area of the bay.	D-133
Figure D.5-17. Habitat distribution in estuary zones for Year 0 and Year 50- 14 km scenario.	D-135
Figure D.5-18. Habitat distribution in estuary zones for Year 0 and Year 50- No Islands scenario.	D-136
Figure D.5-19. Habitat distribution in estuary zones for Year 0 and Year 50- 7 km scenario.	D-137
Figure D.5-20. Cumulative HSI values for shrimp, blue crab and hard clam.	D-138
Figure D.5-21. Cumulative HSI values for oyster, Rangia clam, pompano and bull shark.	D-139
Figure D.5-22. Cumulative HSI values for mackerel, sturgeon, flounder and sea trout.	D-140
Figure D.5-23. Cumulative HSI values for menhaden, croaker, red drum and spot.	D-141
Figure D.6-1. Sketch diagram illustrating conceptual model approach.	D-145
Figure D.6-2. Cross sectional definition sketch of parameters used for shoreline change calculation (after Kraus and Gravens 1991).	D-146
Figure D.6-3. Examples of a few measurable geomorphological indicators of sediment sources and sinks that occur in Louisiana barrier island systems.	D-148
Figure D.6-4. Example of measured Doc based on offshore sediment distribution and profile slope change at Holly Beach, Louisiana Chenier Plain.	D-151
Figure D.6-5. Average profiles for Chalant Pass to Pass de la Mer and Pelican Island, Plaquemines shoreline, Louisiana.	D-152
Figure D.6-6. Equilibrium profile shapes for two hypothetical beaches containing fine sand (0.1 mm ('A'=0.063) and 0.2 mm ('A' = 0.100).	D-153
Figure D.6.7. Hypothetical schematic drawing showing a sand barrier island. A distinction is made between the steeper sand portion of the profile and the flatter mud-dominated portion.	D-154
Figure D.6-8. STWAVE simulation for the Barataria-Plaquemines shoreline, SE Louisiana showing wave decay across the continental shelf.	D-156
Figure D.6-9. Types of nourishment as a function of fill location.	D-159
Figure D.6-10. Illustration of the common components of a subaerial beach nourishment (Type B) and the adjustment expected after initial construction.	D-160
Figure D.6-11. Schematic diagram illustrating the two dominant processes (lateral spreading and cross-shore equilibration) in the design and performance of most beach nourishment projects (after NRC 1995).	D-163
Figure D.6-12. Generic profile types as a function of grain size (after Dean 1991).	D-164

Figure D.6-13. Hypothetical example of longshore spreading of beach fills on an open coast.	D-165
Figure D.6-14. Seawall built to protect a beach-front hotel in Panama City, Florida on the gulf coast (Panhandle). Picture taken in 1998 before the construction of the Panama City Beach Erosion Control and Storm Damage Reduction project.	D-170
Figure D.6-15. Recently built rubble mound revetment at East Timbalier Island (looking east).	D-172
Figure D.6-16 Terminal groin on Captiva Island, Florida southwest Gulf Coast. The beach fill is located to the left of the photograph and Blind Pass is shown to the right.	D-173
Figure D.6-17. Typical groin field (extracted from Douglas 2002).	D-175
Figure D.6-18. Segmented breakwater system of Holly Beach, LA shortly after the beach nourishment (March, 2003 photo taken by Victor Monsour's Photograph, Inc.).	D-176
Figure D.6-19. Empire Jetties located on the SE segment of the Plaquemines shoreline. The picture on top shows remnants of downdrift barrier islands severely eroded, breached, and located away and landward from the jetties. Note: on the land loss map (bottom figure), the pre-existing Shell Island was severely eroded after jetty placement (between 1973 and 1988).	D-178
Figure D.6-20. Dune-building grasses in the southeastern United States	D-181
Figure D.6-21 Conceptual diagram showing the benefits of including a fertilization regime in barrier island vegetative plantings, particularly dune plantings where the sands are extremely nutrient deficient.	D-182
Figure D.6-22 Plant species used in barrier island restoration	D-186
Figure D.7-1. Diagram showing the primary features of a fluvial and deltaic depositional system.	D-190
Figure D.7-2. Map of fluvial channels that developed on the western Louisiana shelf during the most recent sea-level low (from Suter et al. 1987).	D-191
Figure D.7-3. Generalized diagram of the sand-rich shoreline depositional systems discussed in the text.	D-194
Figure D.7-4. Base map showing the regional distribution of sand-rich shoals on the continental shelf that have been investigated for their use as potential sand-resource targets.	D-196
Figure D.7- 5. Base map indicating the locations for Figures 6 to 9.	D-198
Figure D.7- 6. Map illustrating the distribution of sand-resource targets located between Vermillion Bay and Point Au Fer	D-198
Figure D.7- 7. Map showing the distribution of sand-resource targets located between Point Au Fer and the Isles Dernieres barrier island system	D-199
Figure D.7- 8. Map indicating the distribution of sand-resource targets located offshore of the Barataria barrier shoreline	D-200

Figure D.7- 9. Map defining the distribution of sand-resource targets located between Vermilion Bay and Point Au Fer	D-201
Figure D.8-1. Proposed two-side nourishment template for the restoration of the eastern flank of Grand Terre Islands, Louisiana Plaquemines shoreline.	D-207
Figure D.8-2. Relationships between volumetric loss and shoreline retreat for mainland beaches and barrier shorelines (after Dean 1991).	D-208
Figure D.8-3. Pictures depicting the exposure of fine sediments and marsh vegetation on the Gulf side of the Central Segment of East Grand Terre Island.	D-210
Figure D.8-4. Schematic diagram illustrating barrier island volumetric losses (only applicable for barrier islands where minimum beach and dune cross-sections exist).	D-211
Figure D.8-5. Illustration of vegetation planted on Grand Terre Island. Photographs taken in August 2001, courtesy of Darin Lee, Louisiana Department of Natural Resources.	D-216
Figure D.8-6. Location of major Gulf outlets (navigation channels) regularly maintained by the U.S. Army Corps of Engineers, New Orleans district. Beneficial material from these channels is recommended for restoration of back barrier slopes and marshes and creation of new marsh habitats (“spoil islands”).August 2001, courtesy of Darin Lee, Louisiana Department of Natural Resources.	D-217
Figure D.8-7. Beach fill placed in conjunction with stabilizing structures on an open coast, or coasts adjacent to inlets (A) and the recent beach nourishment project built to enhance breakwater performance at Holly Beach, Louisiana (B).	D-218
Figure D.8-8. Raccoon Island detached breakwaters, picture taken in September 2001.	D-220
Figure D.8-9. Schematic diagram illustrating the strategy proposed by Campbell and Jenkins (2001) to stabilize an erosional area and minimize downdrift erosion.	D-220
Figure D.8-10. Dune fencing designs that have been used along the various U.S. coasts.	D-221
Figure D.9-1. Typical components of a low template and landward construction of a barrier island illustrating equilibration of the contained fill after dike removal.	D-223
Figure D.9-2. Typical components of a barrier island restoration using higher templates and seaward and landward construction where the construction and design (equilibrated) templates and the advanced fill are illustrated.	D-224
Figure D.9-3. Dune height of recently built and proposed restoration projects in the Louisiana barrier islands. Italicized numbers indicate dates of construction for constructed projects.	D-226
Figure D.9-4. Illustration of mud profile response to a wave episode (after Mehta 2002).	D-228
Figure D.9-5. Cross-sectional profile located on the western flank of Trinity Island illustrating a relatively low (about 6 ft) protective dune, profile measured by Ritchie et al. (1989). Note the presence of a 30 ft beach berm seaward of the dune crest.	D-230
Figure D.9-6. Protective dunes artificially built at Grand Isle. The dunes were built at higher elevations to avoid overwash and sheet flow across the island and to serve as a storm buffer that would protect island infrastructure.	D-231

Figure D.9-7. Hypothetical non-dimensional diagram illustrating the concept of artificial protective dunes and berms.	D-232
Figure D.9-8. Storm recovery berm verified on Grand Terre Island (picture taken on 07/08/2003) showing onshore-offshore transport of sand.	D-232
Figure D.9-9. Cross-section profile of the submerged segment of the eastern flank of Caminada-Moreau Headland (the Caminada Spit).	D-233
Figure D.10-1. Flow chart illustrating the four design approaches proposed to restore Louisiana barrier islands.	D-235
Figure D.10-2. Geographical location of the Chandeleur Islands and passes.	D-239
Figure D.10-3. The Chandeleur Islands hours after hurricane Georges on Sept. 29, 1998..	D-239
Figure D.10-4. Diagrammatic sketch showing primary dimensional components, boundaries, sediments, and operational slopes for the Chandeleur Islands.	D-242
Figure D.10-5. Strategies proposed for the Chandeleur Islands.	D-243
Figure D.10-6. Geographical location of the Plaquemines barrier islands and inlets/passes.	D-245
Figure D.10-7. Low-lying fragmented barrier island backed by man-made canals in the central Plaquemines shore, between Pass de la Mer and Chaland Pass.	D-246
Figure D.10-8. Diagrammatic sketch showing primary dimensional components, boundaries, sediments, and operational slopes for the Plaquemines Islands.	D-247
Figure D.10-9. General strategies proposed for the Plaquemines shoreline.	D-250
Figure D.10-10. Geographic location of Grand Isle and Caminada-Moreau Headland and associated inlets/passes.	D-253
Figure D.10-11. The coast at the northwestern segment of the Caminada-Moreau Headland showing small salients behind a breakwater field (center of image), a small downdrift erosional feature with small overwashes (top right) and the presence of industrial infrastructure and the Port Fourchon (center and top left) oil and gas production facilities.	D-254
Figure D.10-12. Color infrared image of the eastern end of Grand Isle illustrating island geomorphology (e.g. curved spit) and the presence of private and industrial infrastructure.	D-256
Figure D.10-13. Diagrammatic sketch showing primary dimensional components, boundaries, sediments, and operational slopes for Grand Isle.	D-257
Figure D.10-14. Diagrammatic sketch showing primary dimensional components, boundaries, sediments, and operational slopes for the Caminada-Moreau Headland.	D-256
Figure D.10-15. Proposed strategies for the Lafourche shoreline.	D-258
Figure D.10-16. Geographic location of Timbalier Islands and associated passes.	D-261
Figure D.10-17. Color infrared images of East Timbalier Island illustrating general geomorphology and presence of oil and gas production facilities in the back bay.	D-261
Figure D.10-18. Area change (in acres) for Timbalier and East Timbalier Islands over the	

last century.	D-262
Figure D.10-19. Diagrammatic sketch showing primary dimensional components, boundaries, sediments, and operational slopes for the Timbalier Islands.	D-264
Figure D.10-20. Proposed strategies for East Timbalier and Timbalier Islands.	D-265
Figure D.10-21. Geographic Location of the Isle Dernieres (Raccoon, Whiskey, Trinity \and East Islands) and associated inlets.	D-268
Figure D.10-22. Island area change for the Isles Dernieres during the last century.	D-270
Figure D.10-23. Diagrammatic sketch showing primary dimensional components, boundaries, sediments, and operational slopes for the Isles Dernieres.). The Figure D.10- is vertically exaggerated 50 times for display purposes.	D-271
Figure D.10-24. Digital terrain model of the as-build surveys of the Whiskey Island restoration project.	D-274
Figure D.10-25. General programmatic strategies proposed for the Isle Dernieres.	D-276
Figure D.10-26. Geographic location of the coast between Point Au Fer and Marsh Island.	D-280
Figure D.10-27. Satellite image of Atchafalaya Bay showing the infusion of fine-grained sediment into the bay with decreasing suspended sediment concentrations towards the Gulf of Mexico	D-282
Figure D.10-28. Bathymetric map of the Atchafalaya Bay and inner shelf prior to the gradual dredging of oyster reefs (top) and bathymetric map of the inner shelf and Atchafalaya Bay area after removal of oyster reefs (bottom).	D-283
Figure D.10-29. Marsh Island hydrologic restoration project showing project area and primary land-water features.	D-284
Figure D.10-30. Proposed general management practices for the coast between Point Au Fer and Freshwater Bayou.	D-286
Figure D.10-31. Geographic location of the coast between Freshwater Bayou and Calcasieu Pass.	D-287
Figure D.10-32. Formation mechanisms of cheniers, from Hoyt (1969).	D-288
Figure D.10-33. Incised paleo-channels on the western Louisiana shelf (Berryhill 1986).	D-290
Figure D.10-34. Proposed management practices for the coastal segment located between Point Au Fer and Freshwater Bayou.	D-291
Figure D.10-35. Geographic location of the western Chenier shoreline.	D-293
Figure D.10-36. Construction of the Holly Beach project. Note the dredge delivery pipes on the upper portion of the photograph.	D-294
Figure D.10-37. Proposed management strategies for the western Chenier shoreline.	D-295
Figure D.10-38. Incised paleo-river channel located on the western Louisiana shelf offshore Peveto beach.	D-297

LIST OF TABLES

Table D.2-1.	Summary of offshore wave data for the Louisiana coast.....	D-15
Table D.2-2.	Factors Affecting Storm Severity.....	D-22
Table D.2-3.	Storm Rating based on the Saffir-Simpson Scale.....	D-24
Table D.2-4.	Longshore Sediment Transport Rates for Coastal Louisiana.....	D-35
Table D.3-1	Coast- wide Shoreline Change Rates for Louisiana.....	D-45
Table D.3-2.	Shoreline Data Sources: 1855 to 2002.....	D-56
Table D.3-3.	Louisiana Shoreline Change Geomorphic Regions	D-57
Table D.3-4	Louisiana Shoreline Reaches, Lengths, and Parishes	D-65
Table D.3-5	The Long-term (1855-1989) and Short- Term (1985-2002) Coast-wide Shoreline Changes	D-66
Table D.5- 1.	The Extent of Habitats for Coastal Louisiana Estuaries (%)	D-116
Table D.5- 2.	List of species and variable(s) used to compute habitat suitability index.....	D-119
Table D.5- 3.	Summary of annual salinity differential for each study wit respect to the base case.....	D-120
Table D.5- 4.	Summary of annual salinity differential for each study with respect the base case.....	D-124
Table D.5- 5.	Initial habitat composition for conceptual basin under base case and scenarios (in percentage).....	D-124
Table D.6-1	Sample of previous mobilization and demobilization cost for some Louisiana barrier island restoration projects.....	D-168
Table D.7-1.	Table D.7-displaying the equivalence of the dimensionless phi grain size scale, metric size measurement, and the grain-size terms of the Wentworth classification scheme (modified from Hobson 1979)	D-188
Table D.7-2.	Measures of sorting used to grain-size analysis. Phi units represent a non- dimensional description of the measure of dispersion about the mean grain size; low values are representative of well-sorted sediments (modified from McManus 1988)	D-189
Table D.7-3	Characteristics of offshore sand resources shown in Figures 6 to 9 (from Penland et al. 1990).....	D-202
Table D.9-1.	Template options originally considered by the LCA team for the subaerial portion of restored coastal segments.....	D-224
Table D.9-2.	Design template options originally considered by the LCA team for the subaerial portion of restore costal segments	D-230
Table D.10-1.	Recent and historical shoreline change (ft/yr) and area change (acres/yr) data for the Chandeleur Islands.....	D-240
Table D.10-2.	Inlet widths for Breton Island Pass and Grand Gosier Pass.	D-240

Table D.10-3. Approximate volumetric densities requirements (in cy/ft) to maintain the Chandeleur Islands at the current configuration (maintenance) and to enhance the islands to some uniform minimal cross-section (retreat and stabilized designs).....	D-244
Table D.10-4. Long-term, short-term and recent shoreline change data for the Plaquemines Islands.	D-248
Table D.10-5. Historical minimal cross-sections (in ft) of major inlets and passes on the Plaquemines shoreline.	D-249
Table D.10-6. Rates of increase of tidal inlets that serve as outlets for the Barataria Bay system.	D-249
Table D.10-7. Approximate volumetric densities requirements (in cy/ft) to restore the Plaquemines barriers to some uniform minimal cross-section (retreat and stabilized designs) and maintain the restored templates (advanced fill).....	D-251
Table D.10-8. Approximate densities proposed for the Plaquemines shoreline by previous restoration plans.	D-251
Table D.10-9. Long-term, short-term and recent shoreline change data for the Lafourche shoreline.....	D-255
Table D.10-10. Length of inlets/passes (in ft) in the vicinity of Caminada-Moreau Headland and Grand Isle.....	D-255
Table D.10-11. Approximate volumetric densities requirements (in cy/ft) to restore the Caminada-Moreau Headland to some uniform minimal cross-section (retreat and stabilized designs) and maintain the restored templates (advanced fill)	D-259
Table D.10-12. Long-term, short-term and recent shoreline change data for the Timbalier Islands. Data extracted from Williams et al (1992) (long-term and short term data sets) and Penland (in press) (recent data sets)	D-262
Table D.10-13. Historical dimensions of main inlets/passes associated with Timbalier and East Timbalier Islands.....	D-263
Table D.10-14. Estimated volume densities (in cy/ft) to restore and maintain Timbalier and East Timbalier Islands.....	D-266
Table D.10-15. Long-term, short-term and recent shoreline change data for the Isles Dernieres.	D-270
Table D.10-16. Historical dimensions of main inlets/passes associated with Isles Dernieres. NA stands for data not available (inlet was non-existent or closed).....	D-271
Table D.10-17. Percent area increase and restoration costs for the recently completed CWPPRA projects.	D-273
Table D.10-18. Volumetric densities used in the Isles Dernieres nourishment projects.	D-275
Table D.10-19. Volumetric needs for enhancement of constructed islands, initial construction of Raccoon Island, and maintenance needs (advanced fill).	D-277

Table D.10-20. Gulf shoreline retreat rates for Point Au Fer and Marsh Island. Data for the period between 1955 to 1978 was extracted from van Beek and Meyer Arendt (1982).....	D-281
Table D.10-21. Short and long-term Gulf shoreline change rates for the eastern Chenier Coast.	D-289
Table D.10-22. Estimated volume needs for initial construction (retreat design) and maintenance 9advanced fill0 of restored areas on the coastal segment located between Freshwater Bayou and Calcasieu Pass.	D-292
Table D.10-23. Long-term (1985-1998) and short-term (1983-1994) Gulf shoreline changes for western Chenier Plain (Penland et al. 2003)	D-294
Table D.10-24. Proposed volumetric densities 9intial fill and advanced fill) in cy/ft for the restoration of the west chenier shoreline.....	D-296

Foreword

This Louisiana Coast-Wide Ecosystem Study (LCA) Report Appendix entitled, “Louisiana Gulf Shoreline Restoration Report” is designed to provide an understanding of the geologic framework and expert opinion on the complex processes that shape Louisiana’s Gulf shoreline. Expert science and engineering guidance is provided to help steer the LCA in the successful implementation of projects and programs that will restore Louisiana’s Gulf shoreline. After the impact of Tropical Storm Isidore and Hurricane Lili during the 2002 hurricane season, the Louisiana Department of Natural Resources – Office of Coastal Restoration and Management (LDNR) established the Louisiana Gulf Shoreline Restoration Science Advisory Team (Shoreline Restoration Team) to provide the best multidisciplinary science advice, guidance, and expert opinion to support the Coastal Wetland Planning, Protection, and Restoration Act (CWPPRA) of 1990 and LCA activity for Gulf coastal restoration in Louisiana. The Shoreline Restoration Team consisted of scientists from Louisiana and the United States.

Between November 2002 and May 2003, the Shoreline Restoration Team met four times to exchange information and discuss important Gulf coast restoration issues associated with CWPPRA and LCA. LADNR Assistant Secretary Randy Hanchey tasked the Coastal Restoration Team to prepare this LCA Appendix Chapter.

Many colleagues contributed to the preparation of this important document. The members of the Shoreline Restoration Team would like to recognize the support of Secretary Jack Caldwell, Assistant Secretary Randy Hanchey, Gerry Duszynski, Dr. Bill Good, Jon Porthouse, and Dr. Ken Duffy of the LADNR. We would like to also thank Col. Peter Rowan, John Saia, Troy Constance, Howard Gonzales, and Tim Axtman of the USACE.

Appendix D is a work product of the Pontchartrain Institute for Environmental Sciences at the University of New Orleans and is sponsored by the LDNR. Appendix D is designed to provide additional support to the LCA effort.

Louisiana Gulf Shoreline Restoration Science Team

Shea Penland, Ph.D.: Co-chair
University of New Orleans
Coastal Geomorphology and Processes

Andrew Beall, MSC.
University of New Orleans
Remote Sensing and Change Analysis

Lindino Benedet, MSC.
Coastal Planning & Engineering, Inc.
Oceanography and Coastal Engineering

DeWitt Braud, MSC.
Louisiana State University
Cartography

Paul F. Connor, Jr.
University of New Orleans
Coastal Geology and Change Analysis

Charles Finkl, Ph.D.
Coastal Planning & Engineering, Inc.
Coastal Science and Engineering

Duncan Fitzgerald, Ph.D.
Boston University
Tidal Inlet Morphodynamics and Hydraulics

Ioannis Georgiou Ph.D.
University of New Orleans
Hydrodynamic Modeling

Mark Hester, Ph.D.
University of New Orleans
Coastal Plant Science

Mark Kulp, Ph.D.
University of New Orleans
Framework Geology, Subsidence Processes

Doug Mann, P.E.
Coastal Planning & Engineering, Inc.
Coastal Engineering

Mike Materne, Ph.D.
Louisiana State University
Coastal Plant Science

Alex McCorquodale, Ph.D.
University of New Orleans
Hydrodynamic Modeling

Thomas Campbell, P.E.: Co-chair
Coastal Planning and Engineering, Inc.
Coastal Engineering

Denise Reed, Ph.D.
University of New Orleans
Coastal Geology and Processes

Don Reiso, Ph.D.
U.S. Army Corps of Engineers
Hydrodynamic Modeling

Enrique Reyes, Ph.D.
University of New Orleans
Ecological Modeling

Harry Roberts, Ph.D.
Louisiana State University
Coastal Marine Geology

Asbury Sallenger, Ph.D.
U.S. Geological Survey
Coastal Erosion and Storm Impact

Alex Sheremet, Ph.D.
Louisiana State University
Coastal Processes

Greg Stone, Ph.D.
Louisiana State University
Coastal Morphodynamics

S. Jeffress Williams
U.S. Geological Survey
Framework Geology and Sea-Level Processes

Xiongping Zhang, Ph.D.
Louisiana State University
Coastal Processes

CHAPTER D.1

REGIONAL GEOLOGY OF SOUTHERN LOUISIANA

Mark A. Kulp and Shea Penland¹

¹*Department of Geology and Geophysics and Coastal Research Laboratory, Pontchartrain Institute for Environmental Sciences, University of New Orleans, New Orleans, LA 70148*

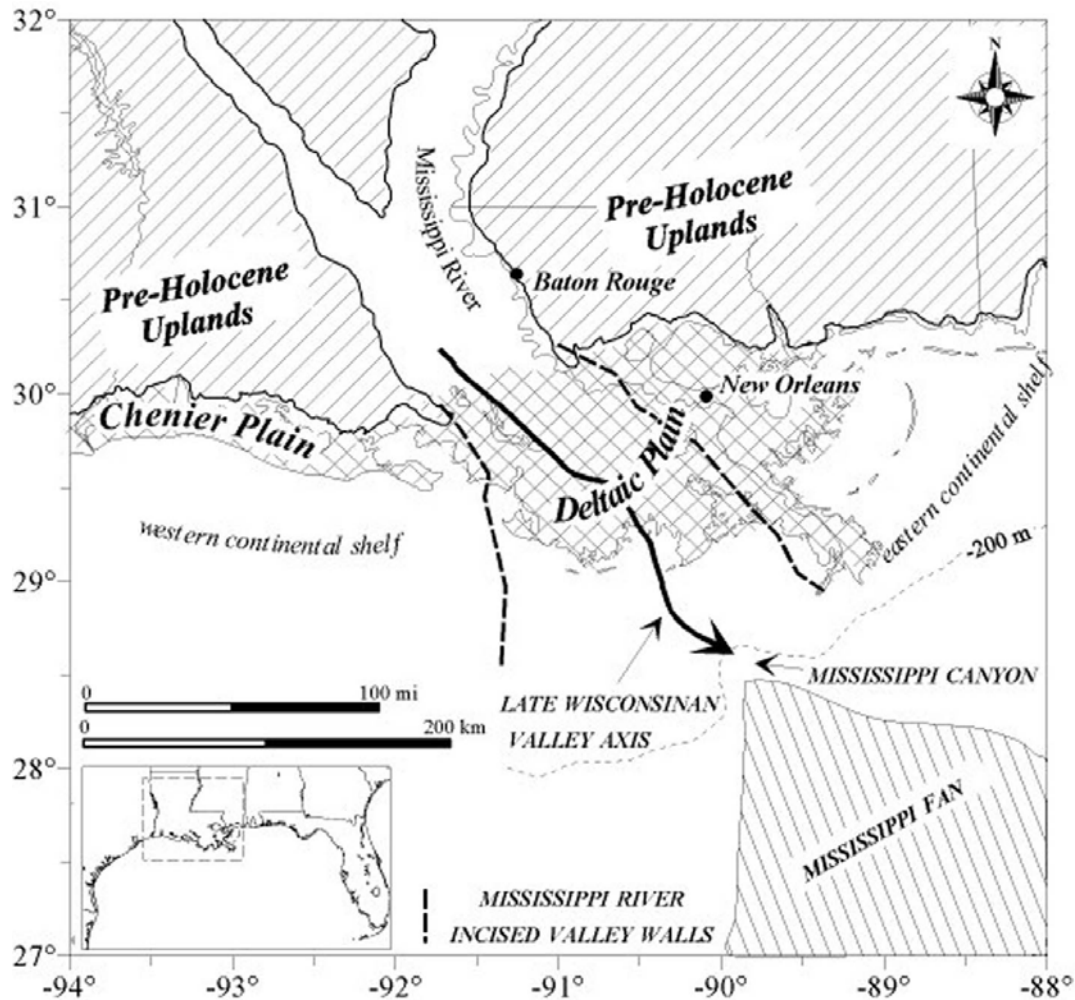
1.1 Summary

This chapter provides an overview of the physiography, structure, stratigraphic framework, and geologic history of southern Louisiana's Mississippi River Delta and Chenier Plain. The intent is to introduce the geologic framework of the region and develop background for topics to be discussed in ensuing chapters. Geologic features and events of the study area, specifically, those of the Holocene (last 10,000 yrs), are given the most emphasis. However, an adequate understanding of contemporary geology is not possible without addressing some regional geologic features and older geologic events.

1.2 Introduction

The north-central Gulf of Mexico basin has been the site of deposition by large fluvial systems since at least the Late Jurassic (~ 150 million years before present (ybp); Mann and Thomas 1968). Since the Late Jurassic, a sedimentary succession in excess of 6 mi thick (10 km thick), deposited in fluvial, deltaic, and marine environments, has accumulated. Through switching sites of major depocenters and progradational outbuilding, the north-central Gulf of Mexico margin has changed considerably. The northern margin of the Gulf basin continues to be the site of major deltaic deposition. Today, the basin receives approximately 6.1 million tons (5.4 million t) of sediment annually from North America's largest drainage basin of more than 1.2 million mi² (3.2 million km²). The trunk distributary of this drainage system is the Mississippi River. During the Holocene, the river constructed the Mississippi River Deltaic Plain, one of the world's largest delta plains in excess of 11,500 mi² (30,000 km²) (Coleman et al. 1998). The Deltaic Plain consists of a generally fine-grained sedimentary package deposited within a wide variety of fluvial, deltaic, and coastal depositional environments. Toward the west, the Deltaic Plain merges with the Louisiana Chenier Plain, an approximately 125-mi long by 12 mi (200-km long by 20-km) coastal plain consisting of sand and shell ridges separated and underlain by mud-rich sediments. The Chenier Plain was formed by processes distinctly different from those responsible for the formation of the fluvial-dominated Deltaic Plain (Figure D.1- 1; Gould and McFarlan 1959; Penland and Suter 1989). Consequently, the Chenier Plain constitutes a physiographic province that, although related to and influenced by Deltaic Plain

processes, is geomorphologically and sedimentologically distinct. The following sections provide a chronologic framework for the formation of the north-central Gulf Basin.



The Mississippi River has, during the Holocene, been confined to an alluvial valley bordered by Pleistocene and older sedimentary units (Pre-Holocene Uplands). Also during the Holocene, the Mississippi River Delta has shifted laterally across the upper continental shelf and constructed a delta plain of more than 30,000 km² (Coleman et al. 1998). Coast-parallel outcrops of pre-Holocene sedimentary units form the northern boundary of the Deltaic and Chenier Plains. The pre-Holocene units dip basinward below the Deltaic and Chenier Plains and are progressively older to the north, perpendicular to their coast-parallel trends (Autin et al. 1991). During the late Wisconsin sea-level lowstand, the Mississippi River extended across the sub-aerially exposed continental shelf (Fisk 1944; McFarlan and LeRoy 1988) delivering sediment to the Mississippi Fan through the Mississippi Canyon (Coleman et al. 1983). The Deltaic and Chenier Plains represent the sub-aerial part of a sedimentary mass deposited by fluvial, deltaic, and marine processes since late Wisconsin sea-level lowstand approximately 18,000 ybp (Coleman et al. 1991). The Chenier Plain, located to the west of the Deltaic Plain, consists of topographically high, sand-rich ridges separated by lower elevation mudflats. Mudflats are progradational in origin, formed by westward-directed longshore drift that transported fine-grained sediment from deltaic depocenters located farther east.

Figure D.1-1. Map of study area showing the Mississippi River Delta region of the north-central Gulf of Mexico.

1.3 Creation and Evolution of the North-Central Gulf of Mexico Basin

The Gulf of Mexico Basin includes south Louisiana. This region was formed by a complex series of geologic processes that began tens of millions of years ago. Within the last 20,000 years, the main landscape-shaping processes have been sediment deposition by the Mississippi River and sea level rise and stabilization.

The Gulf of Mexico Basin is an elliptical, semi-enclosed, depositional basin with a northeast-southwest long axis, bordered by the southern margin of North America and eastern margin of Central America (Figure D.1-1). Open-marine communication is to the Atlantic Ocean between the Yucatan and Florida peninsulas that rim the Gulf Basin on the south and east, respectively.

Formation of the Gulf Basin and its evolution toward a configuration resembling that of today is largely attributed to Late Triassic events initiated by plate tectonics, specifically the break up of Pangea (Salvador 1991). Separation of North America from the African and South American part of Pangea created an extensive network of fault-bounded basins along the southern margin of North America. These basins opened through the early Mesozoic to create the Gulf Basin. Tectonic stability has characterized the basin since the Late Jurassic and led to the development of stable continental shelves and ramps along the basin margins (Salvador 1987). Mesozoic rifting is the most recent plate tectonic event to have affected the Gulf Basin. Subsequent modification of the Mesozoic framework has primarily resulted from accumulation of thick sedimentary successions and basinward outbuilding (progradation) of the post-rift basin margins. Along the north-central basin margin, progradation of Cenozoic depocenters extended the northern margin of the Mesozoic Basin as much as 180 mi (300 km) toward the south.

The result of abundant Cenozoic sediment supply, changing sea level, and migrating depocenters was the deposition of thick clastic sedimentary wedges along the north central basin shelf and slope. The wedges were formed in stacked, imbricated, offlapping depositional packages. Cenozoic sediment thickness is as much as 6 mi (10 km) near the modern Mississippi River depocenter (Galloway et al. 1991). The Cenozoic stratigraphy along the north-central Gulf Basin consists predominantly of interbedded shales, siltstones, and sandstones, deposited in a continuum of shallow shelf to deeper water off-shelf depositional environments.

North-central Gulf Basin depositional patterns during the Quaternary (a subdivision of the Cenozoic) were most strongly influenced by the repeated rise and fall of sea level in response to the growth and decay of Quaternary ice sheets at high latitudes. Along the northern perimeter of the modern Louisiana coastal plain, evidence of these repeated fluctuations in sea level are recorded in successively older, and structurally elevated-to-the-north, “terraces” that dip seaward below Holocene sediments. These sedimentary packages and older units are referred to as pre-Holocene uplands on Figure D.1-1. The more recent Holocene sediments of the Mississippi River Deltaic Plain rest on this foundation.

The most recent lowstand of sea-level elevation occurred during a maximum glacial advance approximately 18,000 ybp (late Wisconsin glacial maximum). Estimates for the elevation of the late Wisconsin sea-level lowstand range between -291 ft and -512 ft (-91 m and -160 m) below modern sea level (Fisk and McFarlan 1955; Curray 1960; Frazier 1974; Suter et al. 1987); however, a -384 ft (-120 m) elevation at 18,000 ybp is generally accepted (Fairbanks 1989; Saucier 1994). Across the outer Louisiana shelf, numerous shelf-edge deltaic intervals

formed during the late Wisconsin phase of falling and low sea level (Suter and Berryhill 1985; Kindinger 1988; Sydow and Roberts 1996). Detailed mapping of these shelf-edge deltaic packages using seismic profile data indicates that progradation of the deltaic packages toward the Pleistocene shelf edge was concomitant with landward erosional truncation and incision of underlying previously deposited sediments as the shoreline shifted basinward approximately 100 mi (~160 km) with the sea-level fall. In areas of minimal incision, this unconformity is preserved in the subsurface as a highly weathered and oxidized surface that resulted from sub-aerial exposure and leaching and has variously been referred to as the Prairie surface or late Wisconsin unconformity (Fisk 1944; Stanley and Warne 1994; Kulp et al. 2002). Fisk and McFarlan (1955) referred to this weathered horizon as the “Prairie surface” because of suggested updip correlation to a coast-parallel outcrop of the late Pleistocene Prairie Formation.

The most prominent late Wisconsin incision was formed as the Mississippi River alluvial valley extended to the shelf edge at the head of the Mississippi Canyon (Figure D.1-1). At the modern coastline, depth to the base of the excavated alluvial valley is approximately 320 ft (100 m). During this sea-level lowstand, much of the river’s sedimentary load was funneled through the Mississippi Canyon to the Mississippi Fan (Figure D.1-1; Coleman et al. 1983). Between 18,000 and 12,000 ybp, delivery of sediments to the shelf edge diminished as sea level rose quickly in response to late Wisconsin deglaciation. Continued sea-level rise and initial flooding of incised valleys created estuaries that favored deposition of fine-grained, organic-rich sediment (Coleman et al. 1983). Relatively coarser-grained, braided fluvial systems that developed during lowstand conditions adjusted to the subsequent sea-level rise by evolving toward meandering regimes (Coleman et al. 1991). As sea-level rose and estuaries flooded, backswamp and floodplain environments developed and deposition within these topographically low areas was enhanced (Kulp et al. 2002). This deposition is recorded in the upward-fining grain size of the relatively coarser-grained substratum interval that fills the zones of late Wisconsin incision. Organic-rich sediments of brackish/estuarine origin above coarse-grained, channel-fill sediments typically indicate initial drowning and inception of estuarine environments within the stream valleys flooded by rising sea level (Suter et al. 1987; Sydow and Roberts 1996). This initial flooding marks a major change in depositional style, generally recorded in the incised valleys as a vertical gradation from gravelly sand sediments to more organic-rich, finer-grained strata. Fisk (1944) referred to the generally fine-grained unit above substratum and interfluvies as topstratum. The topstratum sediments record marine, deltaic, and low-gradient fluvial deposition within formerly incised valleys, as well as on the continental shelf (e.g. Fisk and McClelland 1959). Approximately 12,000 to 10,000 ybp, rates of sea-level rise had slowed enough to allow the Mississippi River to begin prograding outward from the confines of the southern terminus of the alluvial valley onto the bordering continental shelf and begin forming the Mississippi River Deltaic and Chenier Plains of southern Louisiana.

1.4 Holocene Evolution and Physiographic Provinces

1.4.1 Formation of the Deltaic and Chenier Plains

The Holocene geologic framework and history of the Mississippi River Deltaic Plain and bordering Chenier Plain have been determined from more than 30,000 borings, high-resolution seismic reflection profiles, and hundreds of radiocarbon age determinations. Current depositional models describe the Holocene history of the Mississippi River Delta as a dynamic, multi-stage process that reflects the complex interplay between changing rates of sea-level rise and sediment fluvial dispersal pathways (Frazier 1967; Penland et al. 1988; Boyd et al. 1989). The Holocene sedimentary package contains depositional units that have developed as a result of deltaic progradation and abandonment, resulting in an assemblage of overlapping, stacked units of unconsolidated sands and muddy sediments. Growth and abandonment of these deltas are responsible for the formation of the Deltaic Plain in the central and southeastern portions of coastal Louisiana and contributed directly to the formation of the Chenier Plain to the west (Figures 1).

1.4.2 Deltaic Plain

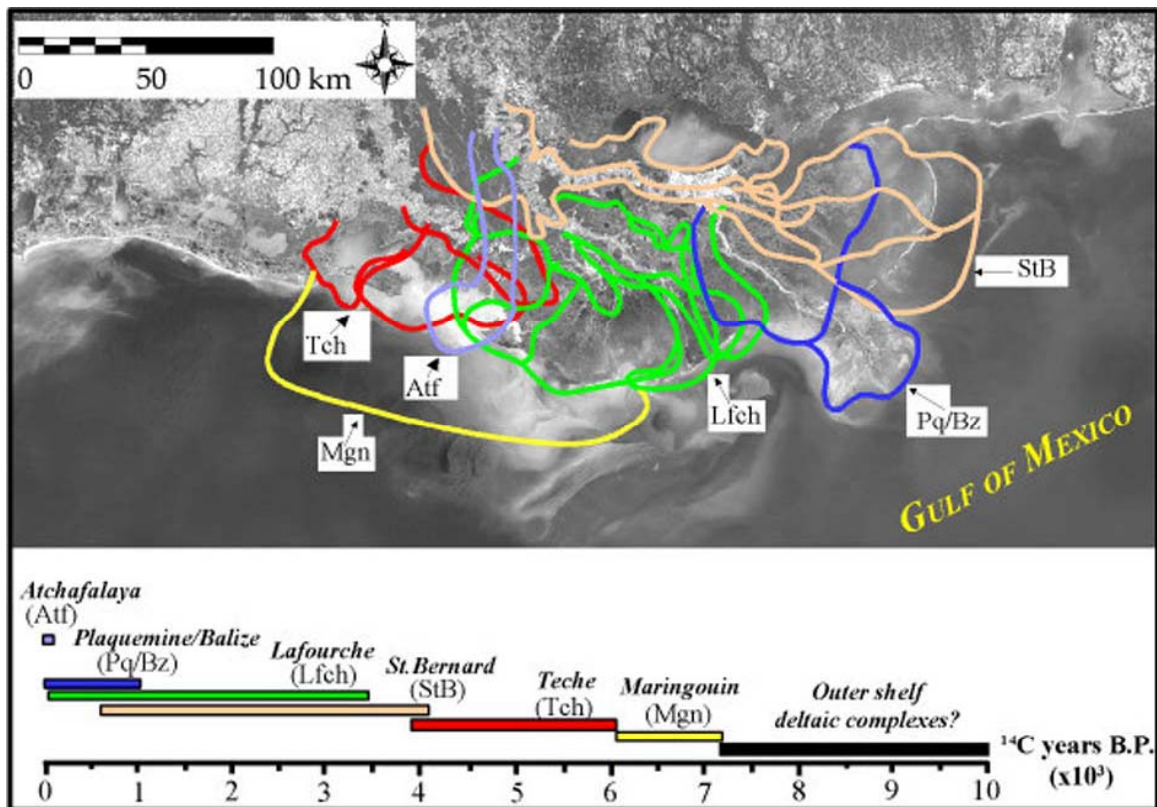
South Louisiana consists primarily of sediments deposited by the Mississippi River as it emptied into the Gulf of Mexico over the last 10,000 years. The river has altered its course many times, causing mud-rich sediment to be accumulated in a variety of locations across south Louisiana and creating the modern Mississippi River Deltaic Plain.

The modern Mississippi River Deltaic Plain consists of two active (Balize and Atchafalaya depocenters) and several inactive deltaic complexes (Figure D.1-2). Each time the Mississippi River has built a major delta lobe seaward at the front of a seaward advancing distributary network (regressive deposition), it has subsequently been abandoned in favor of a shorter, more direct route to the sea. Changes in distributary courses and the accompanying shifts in sites of deposition have resulted in the geographic distribution of deltaic sediments along the coast of southeast Louisiana. Soon after a delta lobe is abandoned, marine inundation and reworking of the delta (transgression) begin as a result of decreased sediment supply and substrate subsidence. Individual deltaic complexes generally undergo a regressive phase of deposition that lasts approximately 1,000 to 2,000 years. These alternating cycles of regression and transgression, driven by delta lobe growth and lobe abandonment and marine reworking respectively, have been termed the delta cycle (Figure D.1-3) (Scruton 1960; Roberts, 1997). The delta cycle has been of fundamental importance to the construction of the southern Louisiana fluvial, deltaic, and barrier shoreline environments and landscape.

Regressive Episodes

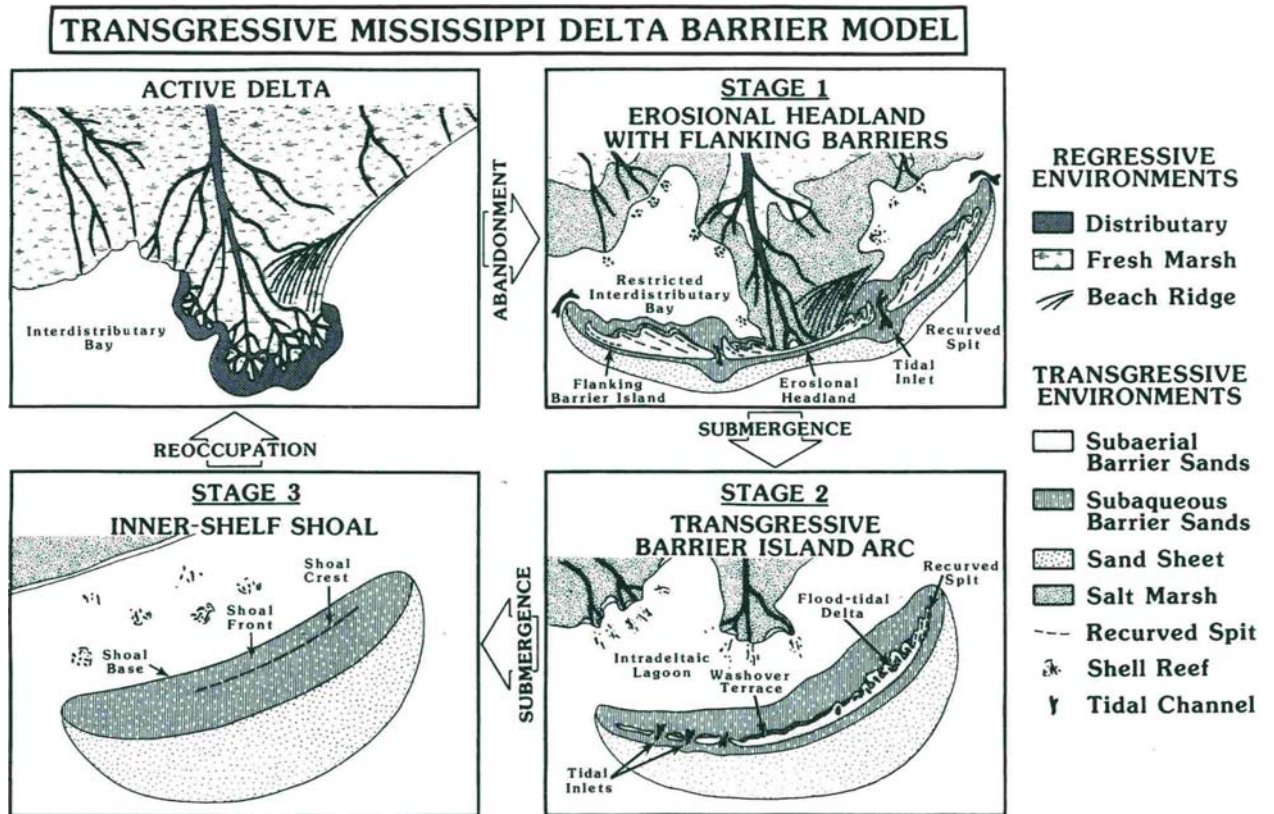
Regressive deposition is recognized as an important process contributing to the vertically stacked and laterally offset deltaic depocenters that are preserved within the shallow Holocene stratigraphic framework of the Mississippi River Deltaic Plain and adjacent continental shelf (e.g. Scruton 1960; Coleman and Gagliano 1966; Frazier 1967). Regressive depositional episodes are characterized by the seaward advance of distributaries, resulting in the construction of deltaic headlands and a progressively more seaward coastline. During regressive sedimentation, prodeltaic sediments at the head of the advancing deltaic front form a mud-rich platform across which the distributaries advance. This process results in a progressively

coarsening upward sedimentary unit that typifies deltaic progradation. Moreover, during deltaic progradations, wetlands fringing the deltaic front and distributary network expand laterally, creating a landscape dominated by fluvial pathways, wetlands, and bays between active distributary networks. Distributaries are, however, ephemeral; seaward progradation results in lengthened distributary networks, a reduction in their gradient, and ultimately, abandonment of the active distributary networks in favor of shorter, more hydraulically efficient routes. Distributary switching is a naturally occurring event and a fundamental process that has contributed to the overall geomorphology and architecture of the Holocene Mississippi River deltaic sediments.



By at least 10,000 ybp deltaic sequences were being constructed on the upper shelf during times of relative sea-level stability in the overall rising sea level (Boyd et al. 1989). Following sea-level highstand at approximately 4,000 ybp, deltaic progradation switched to the east, migrating through distributary switching processes to the west and eventually to the modern Birdfoot Delta (Balize depocenter). Net result of the migrating depocenters is a vertically stacked and offset sedimentary package of primarily deltaic deposits that have created the extensive fluvial networks and wetlands of southern Louisiana. Following abandonment of individual delta lobes the deltaic depocenters became submerged and reworked by marine processes. The depocenters then formed transgressive coastlines, barrier island systems, and ultimately submerged sand shoals on the continental shelf. Chronology and distribution of deltaic complexes modified from Frazier (1967).

Figure D.1-2 Geographic distribution and chronology of Holocene Mississippi River delta



Abandoned erosional headlands built by seaward-advancing delta lobes are subject to marine reworking, resulting in transgression and their ultimate transformation to a inner-shelf, sand-rich shoal (from Penland et al. 1988).

Figure D.1-3. Three-stage conceptual model detailing the genesis and evolution of transgressive depositional systems along the Mississippi River Deltaic Plain

Since the seminal work of Fisk (1944), in which he recognized six delta complexes consisting of smaller subdeltas or delta lobes, several chronologic frameworks for the Holocene Mississippi River deltaic deposits have been suggested (e.g. Kolb and Van Lopik 1966; Frazier 1967), although Frazier's (1967) model appears to be most widely accepted. Using a large database of borings and radiocarbon dates, Frazier (1967) identified five delta complexes and a total of 16 delta lobes that are characteristically lobate in shape. A delta complex represents the sedimentary package deposited by all of the smaller delta lobes that are tied to a common distributary. From oldest to youngest, the delta complexes are: the Maringouin, Teche, St. Bernard, Lafourche, and Plaquemine-Balize (Figure D.1-2). Dates highlighting the age of the deltaic depocenters have been derived from radiocarbon-dated deposits (e.g. McFarlan 1961; Frazier 1967; Tornqvist et al. 1996) as well as archeological evidence (McIntire 1954). The timing of distributary switching to produce the lateral offset of each delta complex are not yet fully understood, but apparently the latter three deltaic complexes shared distributary flow at times. Recently Penland and others (1988) recognized above Maringouin and Teche deposits a laterally extensive marine ravinement surface that probably formed during an absolute sea-level rise. Thus, the Maringouin-Teche complexes constitute an early Holocene delta plain constructed during a time of relatively stable sea level. Subsequent sea-level rise reworked and truncated these early deltaic deposits and created a ravinement across which subsequent deltaic complexes

prograded to form the most recent deltaic plain. Except for the modern Plaquemine/Balize deposition located at the shelf edge, the Holocene Deltas were restricted to shallow inner-shelf waters as indicated by their relatively thin (30 ft to 100-ft thick; 10 to 30-m thick) but geographically extensive coverage (as much as 5,400 mi²; 15,000 km²). In contrast, the Plaquemine/Balize shelf-edge package is geographically restricted but consists of an interval of progradational sediments nearly 320-ft thick (100-m) (Kulp et al. 2002).

Transgressive Episodes

Distributary abandonment, coupled with the combined effects of substrate subsidence and absolute sea-level rise results in erosional headland retreat and the landward migration of the shoreline as sediment is reworked and redistributed by marine processes. As the headlands are subjected to wave and storm erosion during a period of diminishing or non-existent sediment supply, the sediment comprising the headland is dispersed laterally and contributes to the construction and nourishment of flanking beaches, beach ridges, and chenier plains. Penland and others (1988) emphasized the significance of headland reworking and transgressive events in the stratigraphic architecture of the deltaic system, through a conceptual model that accounts for the genesis of transgressive stratigraphy. Their three-stage model depicts the evolution of an active deltaic headland to an inner-shelf shoal through processes of marine reworking and relative sea-level rise (Figure D.1-3).

Transgressive deposition begins when marine processes transform an abandoned deltaic depocenter into an erosional headland with flanking headland barriers and re-curved spits built by longshore transport of headland sand sources (Stage 1). Limited sediment supply from the abandoned distributaries coupled with continued relative sea-level rise and shoreface erosion eventually leads to detachment of the stage-1 barrier shoreline from the mainland and formation of a stage-2, barrier-island arc. The final stage occurs during transgressive submergence when the ongoing relative sea-level rise and storm processes rework the barrier island arc sediment and convert it to a sand-rich marine shoal that is separated from the deltaic coastline, ultimately becoming isolated on the inner shelf (Figure D.1-3). This three-stage model explains the overall distribution of active and abandoned fluvial networks on the Deltaic Plain as well as the distribution and relationship of shorelines and barrier island systems that fringe the southern Louisiana coast. The phases of regression and transgression that the Deltaic Plain has undergone during its evolution have been conceptualized within the delta cycle model (Figure D.1-4).

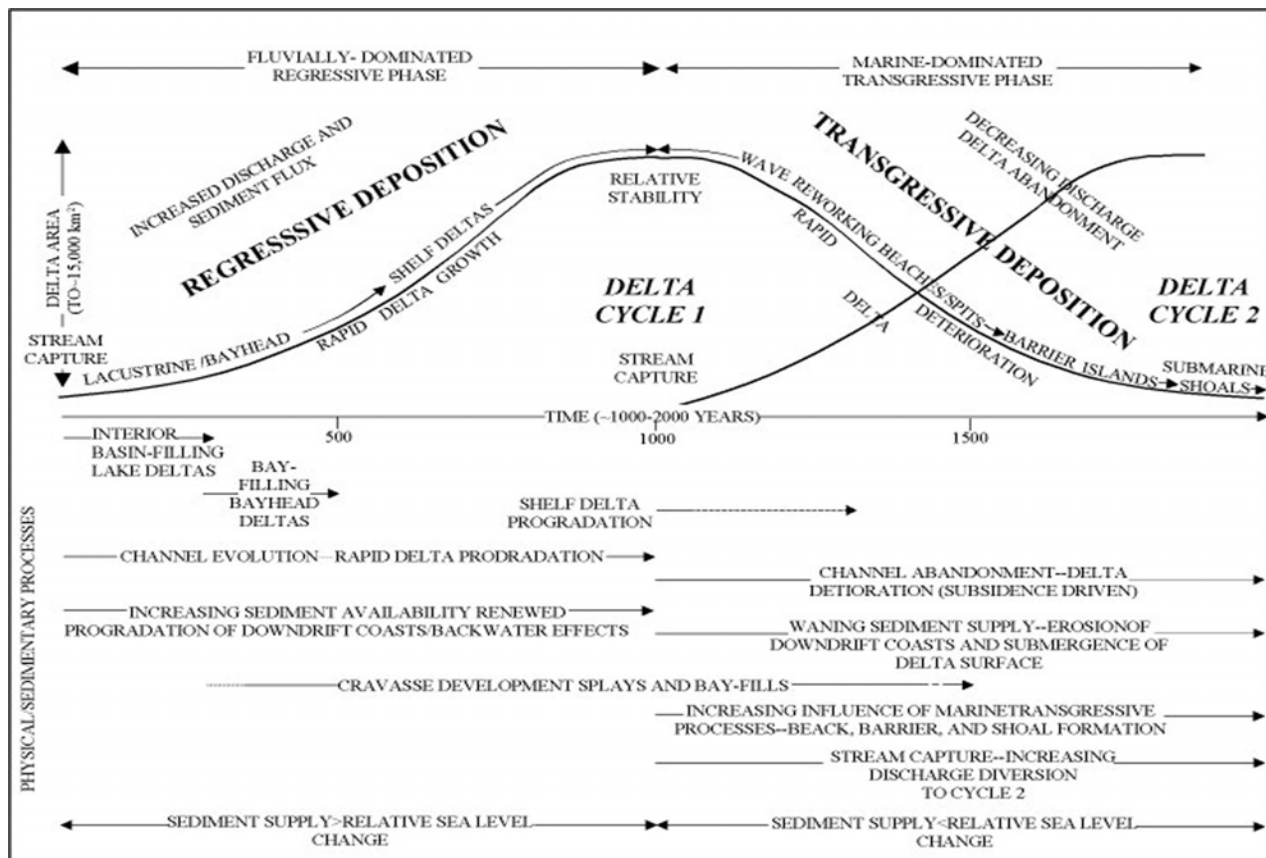
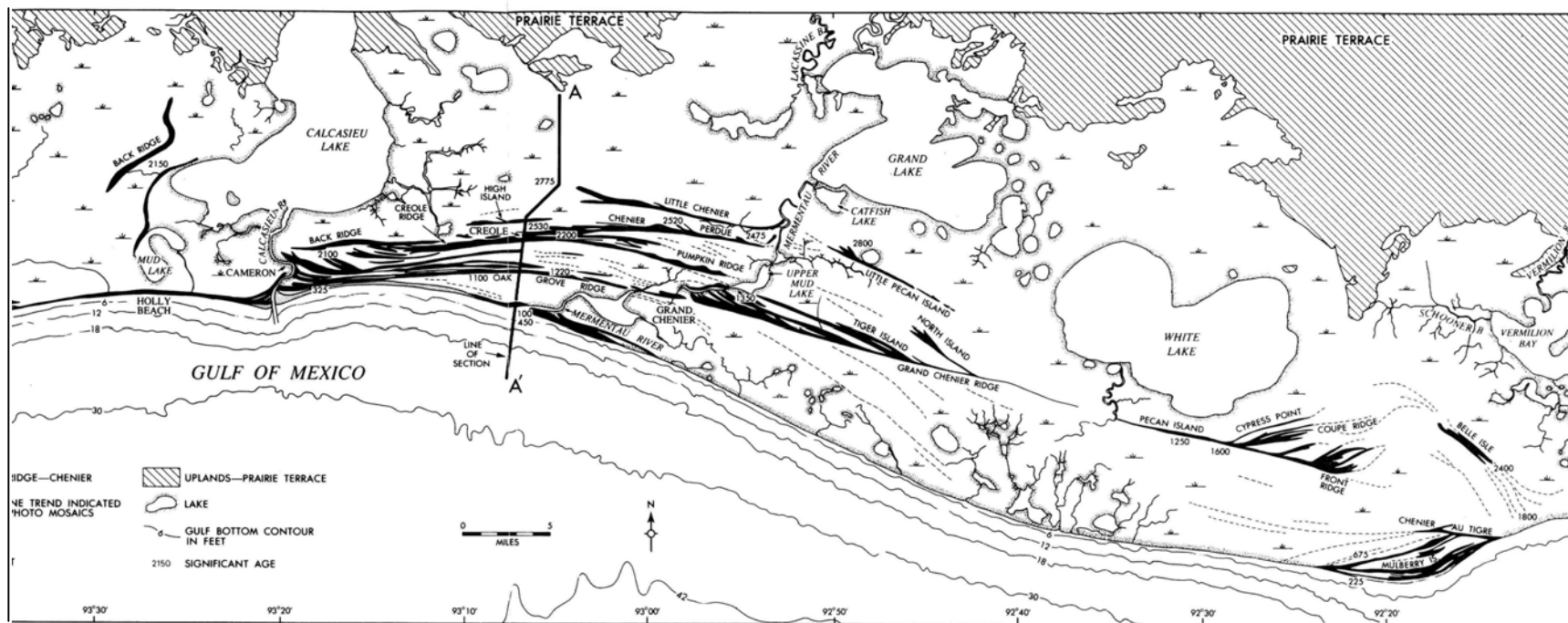


Figure D.1-4. Graph of the delta cycle showing the growth and decay of individual delta lobes through processes of fluvial switching and relative sea level rise (from Roberts 1997).

1.4.3 Chenier Plain

The Chenier Plain was formed by different processes than the Deltaic Plain. Some river sediments were carried west by currents, where they accumulated in broad areas called mudflats. After years of exposure to waves and currents, the mudflats were eventually molded into sandy ridges located parallel to the shore. Oak trees (“cheniers” in French) grew on these ridges and gave the region its name.

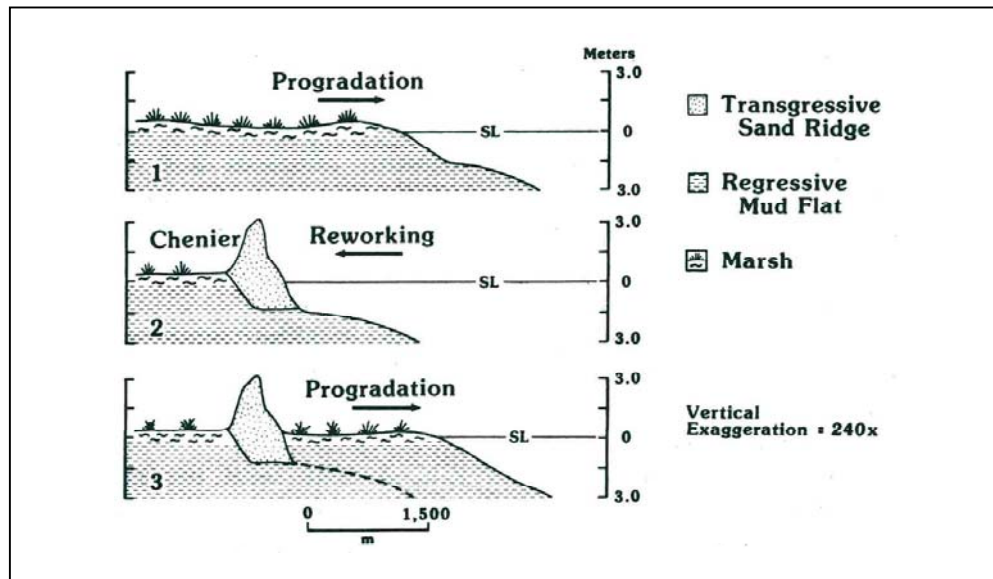
A chenier plain consists of multiple shore parallel, sand-rich ridges that are perched on and physically separated from one another by relatively finer-grained, clay rich sediments (Figure D.1-5). The Chenier Plain of southwestern Louisiana extends from Sabine Pass, Texas to Southwest Point Louisiana, with elevations of approximately 6 to 20 ft (2 to 6 m). The Chenier Plain evolved during the Holocene as a sequence of progradational mudflats that were intermittently reworked into sandy or shelly ridges to form the modern physiography. Numerous cycles of deposition and erosion created alternating ridges separated by marshlands. Sediment of the Chenier Plain has been primarily supplied by longshore transport of fine-grained Mississippi River sediments west of the Deltaic Plain. These sediments, transported by westward flowing nearshore currents, were eventually deposited along the chenier shoreline as mudflats that built seaward with continued sediment supply. When deposition ceased or declined due to a shift in



Note the shore parallel distribution of sandy ridges separated by ridge-elongate mud flats and marshlands. Ages on ridges indicate their radiometrically-determined times of formation (by Gould and McFarlan 1959)

Figure D.1-5. Regional geomorphologic framework of the southwestern Louisiana Chenier Plain.

Mississippi River Delta depocenters on the east, the previously deposited mud-rich sediment was reworked by coastal processes. These processes concentrated the coarse grained sediments and formed shore-parallel ridges called “cheniers” (Gould and McFarlan 1959; Byrne et al. 1959). Introduction of new sediment by westward shifts of the Mississippi River Delta resulted in the isolation of these ridges by accretion of new material on the existing shoreline (Figure D.1-6). Thus, repeated seaward growth and retreat along the Chenier Plain is a consequence of deltaic deposition farther east as well as the periodic cessation of sediment supply to the Chenier Plain as deltaic depocenters were abandoned. Currently, the Atchafalaya River is supplying the Chenier Plain with fine sediments by westward-directed longshore transport of fine-grained material.



. Stage 1 is characterized by mudflat progradation as updrift deltaic lobes prograde seaward and fine-grained sediment at the advancing deltaic front is transported downdrift and accreted along the Chenier Plain, resulting in mudflat progradation. During Stage 2, sediment supply is curtailed as updrift delta lobes are abandoned for other less mature and perhaps more distally located distributaries and delta lobes. As a result, the shoreline is subject to reworking by marine processes. Fine-grained sediment is winnowed from the shoreline, leaving a relatively coarser-grained sand-rich chenier ridge. Renewed progradation of the mudflats occurs as delta lobes begin again to supply fine-grained material to the downdrift Chenier Plain. Because the growth of delta lobes on the Deltaic Plain strongly influences the timing and magnitude of chenier plain progradation and reworking, the growth of the Chenier Plain is very closely tied to the delta cycle and switching model (by Penland and Suter 1989).

Figure D.1-6. Conceptual diagram showing the processes contributing to the construction of the southwestern Louisiana Chenier Plain

1.5 Conclusion

The surface and subsurface geology of the Mississippi Delta region is the byproduct of a complex and varied history related to fluvial, deltaic, and marine sedimentary processes. These processes are influenced by sea-level variations as well as large-scale plate tectonic events. Within the last 10,000 years (Holocene epoch), deposition within a wide variety of fluvial, deltaic, and coastal environments has contributed to the construction of a generally fine-grained sedimentary package that forms the contemporary Mississippi River Deltaic Plain, wetlands, and fringing barrier island systems. West of the Deltaic Plain are the physiographically distinct sand-rich ridges and mudflats of the Louisiana Chenier Plain. Although the Deltaic Plain provided the sediments that built the Chenier Plain, the cheniers were created by different processes than those that govern the fluvial-dominated Delta. The region's geology is complex, but the fundamentals of geologic evolution are reasonably well understood, providing a solid foundation for understanding the processes of coastal change and wetland loss in Louisiana.